Korean J. Chem. Eng., **31**(5), 868-874 (2014)
DOI: 10.1007/s11814-013-0294-2

pISSN: 0256-1115
eISSN: 1975-7220

Factorial design in optimization of the separation of uranium from yellowcake across a hollow fiber supported liquid membrane, with mass transport modeling

Natchanun Leepipatpaiboon*, Ura Pancharoen, Niti Sunsandee***, and Prakorn Ramakul****,†**

*Chromatography and Separation Research Unit, Department of Chemistry, Faculty of Science, Chulalongkorn University, Patumwan, Bangkok 10330, Thailand
**Department of Chemical Engineering, Faculty of Engineering, Chulalongkorn University, Patumwan, Bangkok 10330, Thailand
***Government Pharmaceutical Organization, Ratchathevi, Bangkok 10400, Thailand
****Department of Chemical Engineering, Faculty of Engineering and Industrial Technology, Silpakorn University, Nakhon Pathom 73000, Thailand
(*Received 30 June 2013 • accepted 28 December 2013*)

Abstract−The extraction and stripping of uranium(VI) from other impurity elements in yellowcake was performed simultaneously in one stage by a hollow fiber supported liquid membrane. Uranium ions were selectively extracted from yellowcake using TBP as the extractant, while thorium and some rare earth elements were rejected in the raffinate. The optimization method was carried out using 3^2 factorial design. The concentration of nitric acid in the feed solution and the concentration of TBP in the liquid membrane were regarded as factors in the optimization. A mass transport model focusing on the boundary layer of the extraction side was also applied. The model can predict the concentration of uranium in the feed tank at different times. The validity of the developed model was statistically evaluated through a comparison with experimental data, and good agreement was obtained.

Keywords: Factorial Design, Hollow Fiber, Liquid Membrane, Uranium, Yellowcake

INTRODUCTION

Uranium is known to cause serious environmental damage and acute toxicological effects in mammals, and its compounds are potential carcinogens [1,2]. It has been found in monazite ore in the south of Thailand in the form of phosphate compounds. In the digestion process, monazite ore is broken down using an alkaline process to separate and purify the element. A solvent extraction process has also been used to separate uranium from thorium. Ultimately, uranium is precipitated in the form of ammonium diuranate ($(NH_4)_2U_2O_7$), also known as "yellowcake." However, yellowcake still contains a few impurities of thorium and some rare earth elements (cerium, lanthanum, neodymium, praseodymium, samarium, gadolinium, dysprosium and yttrium), and should be further purified.

Solvent extraction processes have conventionally been employed with various extractants to purify uranium and/or thorium. In the PUREX process [3], TBP (tri-*n*-butylphosphate) is used as the extractant to extract uranium. In the AMEX process [4], thorium is extracted with a primary amine in the first cycle, and uranium is extracted in the second cycle using a secondary or tertiary amine. In the THOREX process [5], 30% (v/v) TBP is used to mutually separate thorium and uranium from 4 M nitric acid solution.

In recent years, other extractants have been used to separate uranium and thorium. Nasab et al. [6,7] used Cyanex302 and Cyanex272 as extractants, and a high separation factor of 3.76 for the separation of thorium from uranium was obtained. Hughes and Singh [8] extracted thorium from monazite sulfate solution by 0.1 M of Adogen-283. Multistage extraction, scrubbing and stripping were performed, and 99.5% yield and 99.86% purity were obtained. Amaral and Morais [9] used a mixture of Primene JM-T and Alamine to selectively extract thorium and uranium from sulfuric liquor by solvent extraction, which was composed of extraction and stripping stages. The result indicated that thorium and uranium extraction was 99.9% and 99.4%, respectively.

However, these solvent extraction processes have some disadvantages because of low selectivity of uranium, consuming large amounts of solvents that are hazardous and flammable. Moreover, multistage extraction and stripping steps must be employed [9,10]. These disadvantages can be avoided if there is a more energy-efficient process to separate uranium and thorium.

Therefore, due to safety and technological considerations, finding a new method to separate and purify uranium from either monazite processing directly or from yellowcake is important.

Hydrometallurgical separation by a liquid membrane process presents a great challenge for the separation of uranium in view of the stringent nuclear waste management regulations. This technique has specific characteristics of simultaneous extraction and stripping in one single stage. It is possible to attain high selectivity [11] employing less energy and input materials compared with other conventional separation methods [12,13].

There are three kinds of supported liquid membrane: flat sheet, spiral, and hollow fiber supported liquid membrane. Some research has been conducted on the separation of uranium by liquid membrane. Kedari et al. [14] separated uranium from thorium solutions

†To whom correspondence should be addressed.
E-mail: prakorn@su.ac.th, korn_mass_transfer@hotmail.com

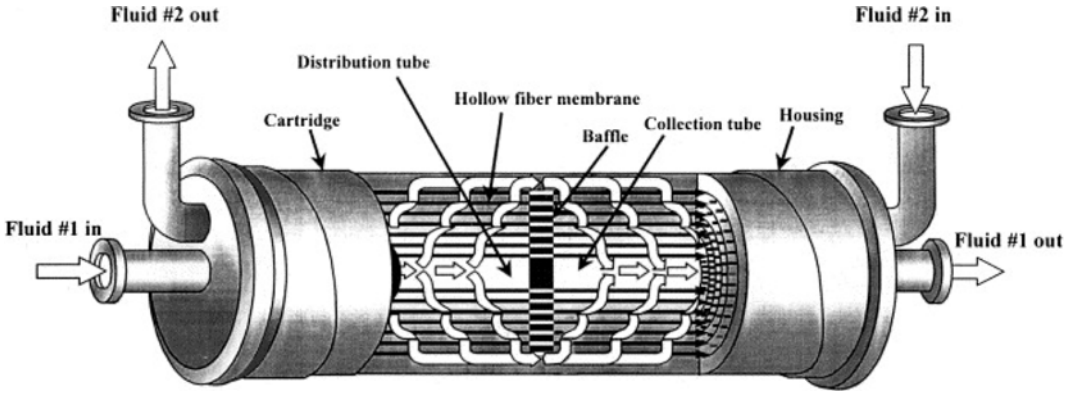

Fig. 1. Hollow fiber supported liquid membrane contactor.

by flat sheet supported liquid membrane. TOPO dissolved in dodecane was used as the extractant. High selectivity of uranium over thorium was obtained. However, this work had no other impurity elements in the feed solution, and a flat sheet supported liquid membrane cannot be applied in continuous mode.

One of the most promising techniques is the hollow fiber supported liquid membrane (HFSLM) because it has no entrainment and flooding, easy to install, high interfacial area, high selectivity, high efficiency for low metal concentrations [13,15,16], and compatibility with other separation techniques [16,18]. In our previous studies, the separation of several kinds of metal ions as well as pharmaceutical products by a hollow fiber supported liquid membrane have been reported [16,19-24].

The experimental design is a way to investigate the entire influence of a given variable, to assess its individual effect as an isolated variable and its interaction with other variables, and also to determine which variable could be neglected. Various experimental designs, such as factorial design, Taguchi design [25], and surface response, have been employed for optimization because they are faster, more economical, more effective, and can simultaneously optimize more than one variable. In particular, factorial design [26,27] is widely used in the statistical planning of experiments to obtain the main factor and optimized condition. Medjahed et al. [28] used full 2^3 factorial design for screening the factors that would influence the experimental results, and also optimized the extraction of copper by supported liquid membrane. The concentration of KSCN was statistically significant, and the optimized percentage of extracted copper(II) was 93.6%. Kavak et al. [29] used full factorial design to screen the factors affecting the efficiency of lead removal by cation exchange resin. Optimization was performed and 99% removal of Pb(II) was obtained.

We demonstrated, for the first time, the separation of uranium from yellowcake solution using a hollow fiber supported liquid membrane. The yellowcake was obtained from monazite ore digestion. Yellowcake dissolved in nitric acid solution typically contains thorium and some rare earths as impurities. The effects of the concentration of nitric acid in the feed solution and the concentration of TBP in the liquid membrane phase were investigated and optimized by using 3^2 full factorial design. In addition, a mathematical model of the process of uranium ion transport across a liquid membrane was studied. The model focused on the transport mechanism and the reaction at the extraction side of the liquid membrane to predict the concentration of uranium in the feed tank at different times. Finally, the theoretical results from the model were compared with experimental data.

BACKGROUND THEORY

1. Hollow Fiber Supported Liquid Membrane

A hollow fiber supported liquid membrane is composed of a module that contains many hollow microporous polyethylene fibers aligned horizontally, as shown in Fig. 1. The fibers are woven into fabric and wrapped around a central tube feeder that supplies the shell-side fluid. The woven fabric allows more uniform fiber spacing, which in turn leads to a higher rate of mass transfer than that obtained with individual fibers. Inside the module, the organic liquid membrane phase is located between the aqueous feed solution, which contains metal ions, and the stripping phase.

2. Separation Mechanism

A liquid membrane is designed to selectively extract only the target metal. The selectivity is controlled by the carrier and form of metal species [30]. We used a feed solution containing uranium(VI), thorium(IV) and some rare earths. TBP (tri-*n*-butylphosphate) as an extractant was used to separate uranium from thorium and other rare earth elements. TBP was dissolved in kerosene as a liquid membrane embedded by capillary force in the hydrophobic microporous hollow fiber module. Uranium in the presence of nitric acid exists in the form of UO_2^{2+} type species [31]. Uranium ions react with TBP at the interface between the feed and liquid membrane to form complex species, according to Eq. (1) [32]:

$$UO_2^{2+} + 2NO_3^- + 2TBP \Leftrightarrow UO_2(NO_3)_2 \cdot 2TBP \quad (1)$$

$$UO_2(NO_3)_2 \cdot 2TBP + 2Na^+ \Leftrightarrow UO_2^{2+} + 2NaNO_3 \cdot TBP \quad (2)$$

After that, the complex species diffuse across the organic liquid membrane to react with sodium hydroxide, as the stripping reagent, at the opposite interface. Then, uranium(VI) ions are stripped into the stripping phase as in Eq. (2), releasing TBP and uranium(VI) into the liquid membrane phase and stripping phase, respectively. Finally, TBP diffuses back to react with the feed phase, in a new cycle where the uranium(VI) ions can once again be extracted and stripped. A schematic diagram depicting the coupled transport between uranium(VI) ions in the feed solution and sodium ions in the stripping solution is shown in Fig. 2.

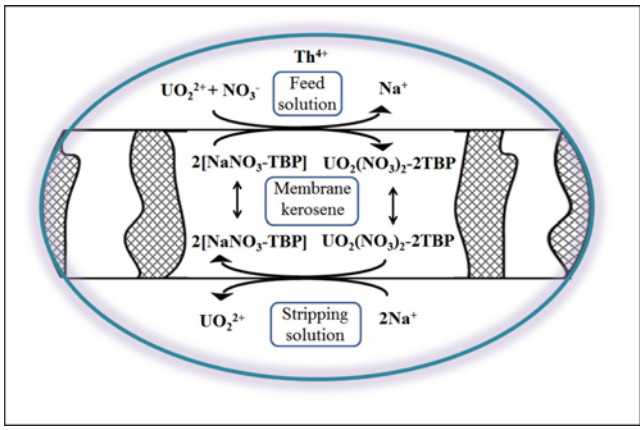

Fig. 2. Transport scheme of extraction and stripping of uranium in a liquid membrane process using TBP.

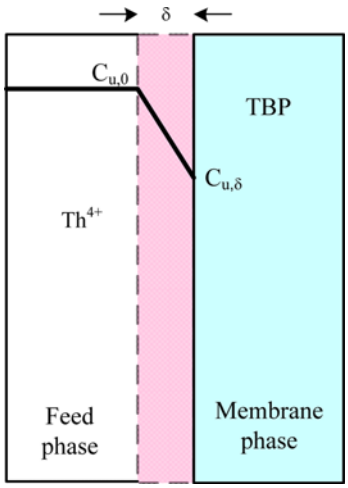

Fig. 3. Schematic representation of concentration profiles and interface layer at the feed side of uranium transport.

3. Mathematical Model Development

A mathematical model of a hollow fiber supported liquid membrane for the separation of uranium ions is illustrated in Fig. 3. The overall mass transport through a liquid membrane is very complicated. Therefore, the following assumptions were applied: (i) the concentration of the feed solution is very low, and all of the uranium ions react with TBP; (ii) bulk uranium ions come in contact with an aqueous boundary layer thickness (δ); (iii) the concentration gradient across the boundary layer is linear; and (iv) the complexation and decomplexation reactions are much faster compared to the diffusion across the boundary layer.

This work focuses on the feed/membrane interface layer, because in most liquid membrane systems the mass transfer controlling step occurs here [30]. All these steps, as a whole, make this phenomenon very complicated. The aqueous feed solution contains uranium ions, while the organic liquid membrane contains a substance, TBP. From the extraction reaction in Eq. (1), at the plane $z=\delta$, UO_2^{2+}, from the feed side moves to react with TBP instantaneously.

Using Fick's (first) law of diffusion, the flux, $N_{U,r}$, is the number of moles of uranium that go through a unit area in unit time, the unit area being fixed in space [33]. The molar flux is related to the concentration gradient, which for the r component is:

$$N_{U,r} = -D_{U,aq}\frac{dC_U}{dr} + x_U N_{U,r} \tag{3}$$

where $D_{U,aq}$ is the diffusivity of UO_2^{2+} in the aqueous phase and is assumed to be constant, while x_u is the mole fraction of UO_2^{2+} in the feed solution.

When the concentration of uranium is low ($x_U \approx 0$), the last term of Eq. (3) is neglected and can be rewritten as:

$$N_{U,r} = -D_{U,aq}\frac{dC_U}{dr} \tag{4}$$

For uranium ion mass balance with a steady-state condition, we obtain Eq. (5):

$$\frac{dN_{U,r}}{dr} = 0 \tag{5}$$

By combining Eqs. (4) and Eq. (5), and integrating with two initial conditions, r=0, $C_U=C_{U,o}$ and $r=\delta$, $C_U=C_\delta=0$, the final equation for the uranium ion concentration can be expressed as:

$$C_U(r) = C_{U,o}\left[1-\frac{r}{\delta}\right] \tag{6}$$

Finally, by substituting Eq. (6) into Eq. (4), we obtain the expression for uranium flux:

$$N_{U,r} = D_{U,aq}\frac{C_{U,o}}{\delta} \tag{7}$$

From the definition of flux [18], we have the following equation:

$$N_{U,r} = \frac{V(C_{U,0}-C_U(t))}{At} \tag{8}$$

By combining Eqs. (7) and (8), the final equation for uranium ion concentration can be expressed as:

$$C_U(t) = C_{U,0}[1-kt] \tag{9}$$

$$\text{where } k = \frac{D_{U,aq}A}{\delta V} \tag{10}$$

Eq. (13) is an equation for predicting the concentration of uranium in the feed tank at different times; the results will be compared with experimental data.

EXPERIMENTAL

1. Reagents

Yellowcake was obtained from the Rare Earth Research and Development Center, Office of Atoms for Peace, Bangkok, Thailand, and was dissolved by HNO_3. The pH of feed solutions was adjusted by NaOH. Tri-*n*-butylphosphate (TBP) was the extractant, kerosene was the organic diluent and NaOH was the stripping solution. All chemicals in the feed solution except yellowcake were of AR grade and purchased from Merck Co. Ltd.

2. Apparatus

- A Liqui-Cel® Laboratory Liquid/Liquid Extraction System (composed of two gear pumps, two variable speed controllers, two rotameters, and two pressure gauges) was used.

Table 1. Characteristics of the hollow fiber module

Properties	Descriptions
Material	Polypropylene
Dimension of module (diameter×length)	6.3×20.3 cm
Inside diameter of hollow fiber	240 μm
Outside diameter of hollow fiber	300 μm
Effective length of hollow fiber	15 cm
Number of hollow fibers	35,000
Average pore size	0.03 μm
Porosity	30%
Effective surface area	1.4×10^4 cm^2
Area per unit volume	29.3 cm^2/cm^3
Module diameter	6.3 cm
Module length	20.3 cm
Contact area	1.4 m^2
Operating temperature	273.15-333.15 K

• A Liqui-Cel® Extra-Flow module offered by Celgard (Charlotte, NC; formerly Hoechst Celanese) was used as a support material. The properties of the hollow fiber module are shown in Table 1. The fibers are potted into a solvent-resistant polyethylene tube sheet with a polypropylene shell casing.

3. Analytical Instruments

• Research reactor for the neutron activation analysis (NAA) method

• Gamma ray spectrometer for the NAA method

4. Procedures

The feed solution was made by dissolving yellowcake in nitric acid, and the liquid membrane was prepared by dissolving TBP in kerosene. The stripping solution was sodium hydroxide. The organic liquid membrane contained TBP, which was allowed to circulate in the tube and shell sides for 20 min. After that, the experiment began by flowing the feed solution into the tube side of the hollow fiber module. Simultaneously, 0.5 M of sodium hydroxide as the stripping solution was countercurrently pumped into the shell side of the hollow fiber module. The experiments were performed in circulation mode. A schematic diagram of the process and a photograph of the instrument used are shown in Fig. 4(a) and 4(b), respectively. For factorial design study, samples (5 mL) were taken out from the feed and stripping tanks at final time of 40 min. In the validation of mathematical model, the sample were taken at 10 min intervals. The concentrations of uranium and thorium ions were measured by the NAA method [34,35]. The experiments were done in quadruplicate, and all of the results were analyzed by 3^2 factorial design.

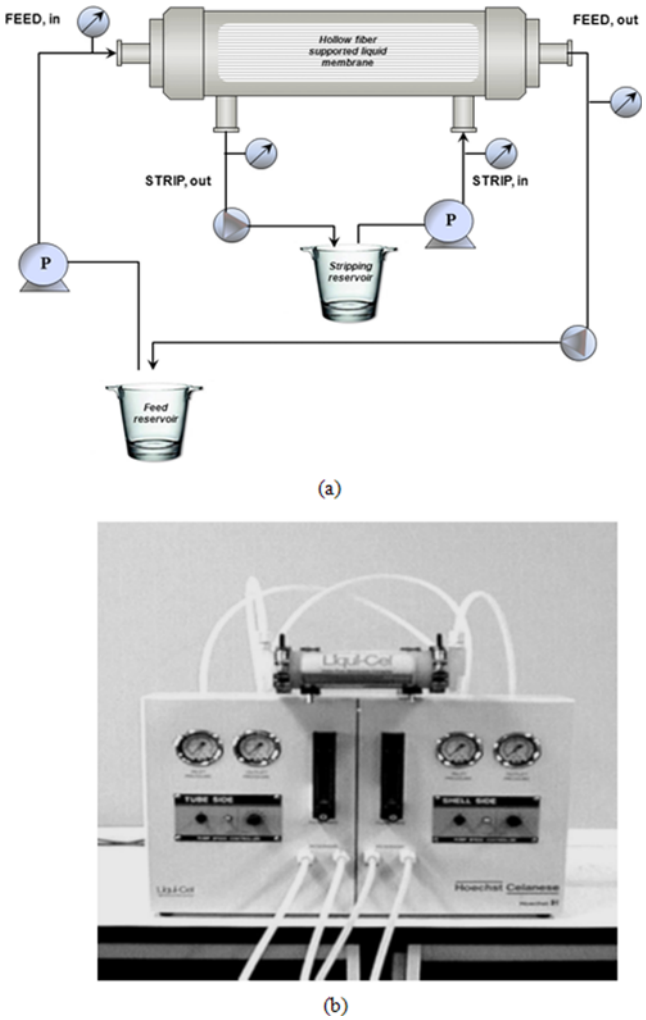

Fig. 4. (a) Schematic diagram of the experimental setup of a hollow fiber supported liquid membrane process; (b) the instruments used for the hollow fiber supported liquid membrane process.

RESULTS AND DISCUSSION

1. Calculation of Aqueous Boundary Layer Thickness

The feed side aqueous boundary layer thickness was calculated by the Lévêque equation [36] considering the laminar flow inside the fibers:

$$sh=\frac{r_i}{\delta}=1.62\left[\frac{d^2v}{LD_{U,aq}}\right]^{1/3} \quad (11)$$

where sh is the Sherwood number, d and L represent the inner diameter and length of the fiber, and v is the linear flow velocity of the feed through the fiber. As can be seen from the above relation, the value of δ depends upon the flow rate of the feed solution.

2. Calculation of Diffusion Coefficient

The diffusion coefficient of the aqueous feed solution, $D_{U,aq}$, was estimated by the Nernst–Haskell equation [37], as in Eq. (12):

$$D_{AB}=\frac{RT[(1/n_+)+(1/n_-)]}{F^2[(1/\lambda_+)+(1/\lambda_-)]} \quad (12)$$

where:

D_{AB}=diffusivity of solute A in solvent B (cm^2/s)

n_+ and n_-=valences of the cation and anion, respectively

λ_+ and λ_-=limiting ionic conductance in (A/cm^2) (V/cm) (g-equiv/cm^3)

F=Faraday's constant (96,500 coulombs/g-equiv)

T=temperature [K]

R=gas constant=8.314 J/mol·K

For some parameters such as temperature (T=300 K), valences

Table 2. Analysis of variance for %extraction of uranium

Source of variation	DF	Sum of squares	Mean square	F	*P*-value
Conc. of TBP (A)	2	612.11	306.06	7.91	0.002
Conc. of HNO_3 (B)	2	2,241.27	1,120.63	28.97	0.000
Interaction (AB)	4	550.81	137.70	3.56	0.019
Error	27	1,044.51	38.69		
Total	35	4,448.7			α=0.05

of the cation (n^+=2) limiting ionic conductance for UO_2^{2+} (λ_+=60.6 A/cm^2) [38]. The diffusivity calculated by the above equation is 1.31×10^{-5} cm^2/s.

3. Factorial Design Study

The selection of the significant variable is very important for determining the optimized condition. To investigate the interaction between the variables in the separation of uranium, 3^2 factorial design was used by varying two important variables: the concentration of TBP in the liquid membrane (A), and the concentration of nitric acid in the feed solution (B). The data of the 3^2 factorial design and the responses are shown in Table 2. Minitab 16.0 software was used to calculate the statistical data, analysis of variance, and the graphs of the 3^2 factorial design study.

From the analysis of variance in Table 2, the *P*-value of the interaction between the concentration of TBP (A) and the concentration of nitric acid (B) is 0.019<0.05. This means that the interaction between these two variables is significant, with 95% confidence. Thus, we can remove the main variables (A and B) from the optimization. The interaction plot of the 3^2 factorial design study is shown in Fig. 5. It can be concluded that 5% (v/v) TBP and 1.0 M of nitric acid are the optimized condition, and they were used for model verification.

4. Uranium Transport and Model Verification

To verify the predictions of the uranium transport model, experiments were performed based on the developed model. The experimental results for different yellowcake concentrations in the feed tank (Fig. 6) and for various flow rates of the feed solution (Fig. 7) were compared with the model predictions.

4-1. Effect of Uranium and Thorium Concentrations in the Feed Solution

Experiments were performed at different feed metal ion concentrations: 200, 300, 400 and 500 ppm. TBP concentration was fixed at 5% (v/v), and sodium hydroxide was used as the stripping solution. According to the experimental results, the rate of uranium transport became slower as the feed concentration increased, because at higher concentrations of uranium ions, fewer TBP molecules are available for extraction. Fig. 6 shows good agreement for the comparison between the experimental and theoretical results obtained by Eq. (9).

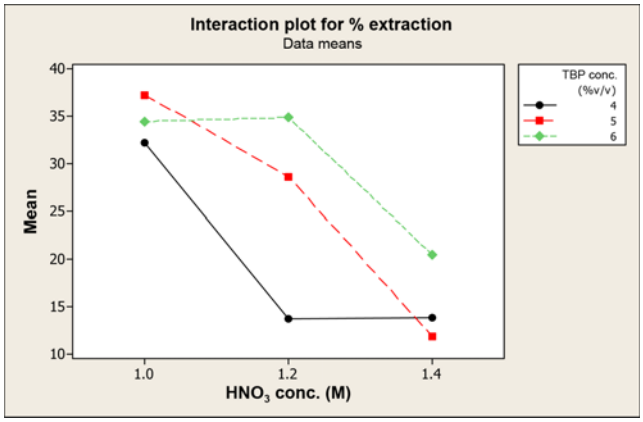

Fig. 5. Plot of the effects of HNO_3 and TBP concentration by 3^2 factorial design, and the responses.

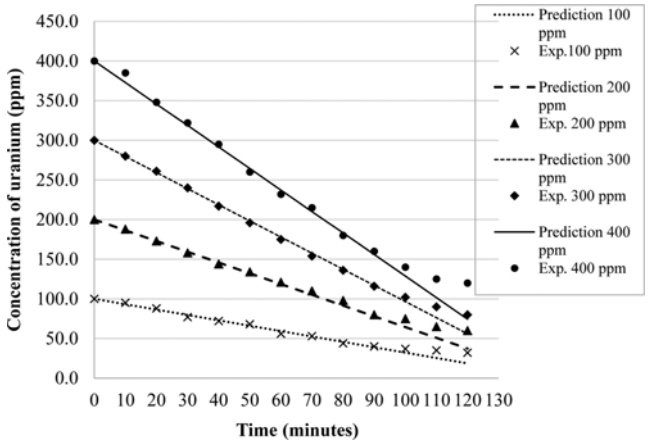

Fig. 6. Effect of initial uranium concentration on the separation rate of uranium. Extractant: 5% (v/v) TBP; stripping solution: 0.5 M NaOH; flow rates of feed and strip: 100 mL/min.

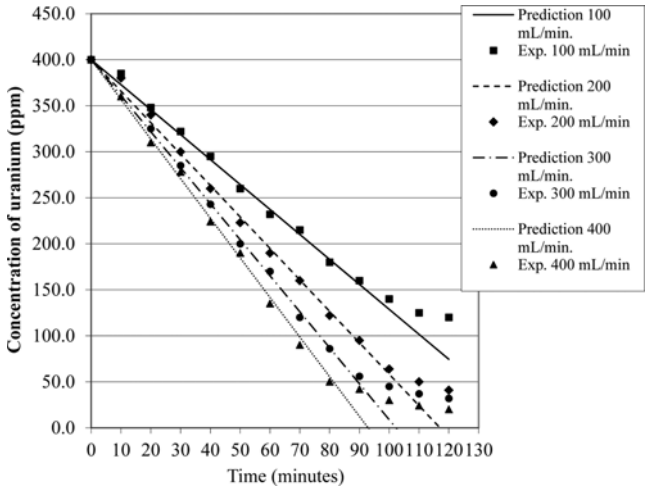

Fig. 7. Effect of flow rate of feed solution on the separation rate of uranium. Extractant: 5% (v/v) TBP; stripping solution: 0.5 M NaOH; flow rate of strip: 100 mL/min.

4-2. Effect of Flow Rate of Feed Solution

A theoretical prediction was also performed to investigate the effect of feed-side flow rate; the experimental and theoretical results are shown in Fig. 7. As the feed flow rate increased from 100-400 mL/min, the slope of the experimental results became more negative. This means that the rate of uranium transport is higher with increasing flow rate of the feed solution. Clearly, the transport model in Eq. (9) can very well predict the concentration of uranium in the feed tank.

According to liquid membrane theory, a higher flow rate means a higher speed of the aqueous phase in the hollow fibers, causing the aqueous boundary layer thickness (δ) to be correspondingly thinner. Consequently, the k value in Eq. (13) is higher; this brings about a lower concentration in the feed tank at final time [22,23], as calculated from Eq. (12).

4-3. Model Verification

The validity of Eq. (9) was checked by comparing with the experimental data. Absolute error percentage (%A.E.), standard deviation (S.D.) and pair *t*-test [39] were used to verify the validity of the mathematical model. A.E. is defined as:

$$\%\text{A.E.} = \frac{|C_{Exp} - C_{Calc}|}{C_{Calc}} \times 100 \tag{13}$$

where C_{Exp} is the concentration of uranium in the feed tank from the experimental result, and C_{Calc} is the concentration of uranium in the feed tank as calculated by the mathematical model. The validity of the mathematical model is also based on the percentage of standard deviation (S.D.) as defined below:

$$\text{S.D.} = \sqrt{\frac{\sum_{i=1}^{N}\left(\frac{C_{Exp}}{C_{Calc}} - 1\right)}{N-1}} \tag{14}$$

where N is the number of experimental data.

The concentrations of uranium in the feed tank as a function of time, for initial feed concentrations of 100, 200, 300 and 400 ppm

Table 3. Comparison between experimental and predicted results and statistical analysis

Time (min)	Feed concentration (ppm)											
	100			200			300			400		
	Exp.	Calc.	A.E.	Exp.	Calc.	A.E.	Exp.	Calc.	A.E.	Exp.	Calc.	A.E.
0	100	100.0	0.000	200	200.0	0.000	300	300.0	0.000	400	400.0	0.000
10	95	93.2	0.019	188	186.4	0.008	280	279.7	0.001	385	372.9	0.033
20	88	86.4	0.018	173	172.9	0.001	261	259.3	0.006	348	345.6	0.007
30	77	79.7	0.033	158	159.3	0.008	240	239.0	0.004	322	318.8	0.010
40	72	72.9	0.012	144	145.8	0.012	217	218.6	0.007	295	291.6	0.012
50	68	66.1	0.029	134	132.2	0.014	196	198.3	0.012	260	264.4	0.017
60	56	59.3	0.056	121	118.6	0.020	175	178.0	0.017	232	237.2	0.022
70	53	52.5	0.009	110	105.1	0.047	154	157.6	0.023	215	210.0	0.024
80	44	45.8	0.038	98	91.5	0.071	136	137.3	0.009	180	183.2	0.017
90	40	39.0	0.026	80	78.0	0.026	116	116.9	0.008	160	156.0	0.026
100	37	32.2	0.149	75	64.4	0.165	102	96.6	0.056	140	128.8	0.087
S.D.		0.0551			0.0598			0.0208			0.0334	
Pair *t*		0.9781			0.8971			0.9893			94662	
Time (min)	Flow rate of feed solution (mL/min)											
	100			200			300			400		
	Exp.	Calc.	A.E.	Exp.	Calc.	A.E.	Exp.	Calc.	A.E.	Exp.	Calc.	A.E.
0	400	400.0	0.000	400	400.0	0.000	400	400.0	0.000	400	400.0	0.000
10	385	372.9	0.033	380	365.8	0.039	385	360.9	0.067	360	356.9	0.009
20	348	345.8	0.006	340	331.7	0.025	325	321.8	0.010	310	313.9	0.012
30	322	318.6	0.011	300	297.5	0.008	285	282.7	0.008	278	270.8	0.026
40	295	291.5	0.012	260	263.3	0.013	243	243.5	0.002	224	227.8	0.017
50	260	264.4	0.017	223	229.2	0.027	200	204.4	0.022	190	184.7	0.028
60	232	237.3	0.022	190	195.0	0.026	170	165.3	0.028	135	141.7	0.047
70	215	210.2	0.023	160	160.8	0.005	120	126.2	0.049	90	98.6	0.088
80	180	183.0	0.017	122	126.6	0.037	86	87.1	0.012	50	55.6	0.101
90	160	155.9	0.026	95	92.5	0.027	56	48.0	0.167	42	12.5	2.349
100	140	128.8	0.087	64	58.3	0.098	45	8.9	4.081	30	−30.5	1.983
S.D.		0.0334			0.0392			1.292			0.9732	
Pair *t*		0.9466			0.9804			0.9136			0.9066	

and flow rates of 100, 200, 300 and 400 mL/min, were predicted. The mathematical model results in Figs. 6 and 7 are shown by the line which fitted well with the experiment data from 0 to 100 min. Table 3 shows the results of %A.E, S.D. and pair *t*-test in the different conditions. The two-tailed pair *t*-values are between 0.9 and 1.0. Therefore, all pairs are less than the significance level of 0.10, which means that the calculation by the mathematical model is acceptable.

Unfortunately, when the flow rate was high, the rate of transport of uranium abruptly decreased, which was not in agreement with the calculated results. This decrease occurred because when the flow rate was too high, i.e., 400 mL/min, the liquid membrane leaked out of the pores and the liquid membrane system was destroyed [22].

CONCLUSION

Hollow fiber supported liquid membrane process can extract and strip uranium(VI) ions from yellowcake solution in a single stage. By 3^2 factorial design, the interaction between the concentration of HNO_3 in the feed solution and the concentration of TBP in the liquid membrane is significant; the optimized conditions are 1.0 M and 5% (v/v), respectively. The rate of uranium transport increased as the flow rate of the feed solution increased, but the transport rate was slower when the feed concentration was increased. An uncomplicated equation was created by mass transfer theory, which can predict the concentration of uranium ions in the feed tank at different times.

ACKNOWLEDGEMENTS

The authors greatly appreciate the financial support from the Thailand Research Fund (TRF) and the Commission on Higher Education as well as Silpakorn University Research and Development Institute. We also wish to thank the Department of Chemical Engineering, Faculty of Engineering, Chulalongkorn University, Thailand, for chemical and apparatus support. The authors would like to thank the Rare Earth Research and Development Center for yellowcake and the Office of Atoms for Peace, Bangkok, Thailand, for the measurement of concentrations of uranium and thorium by NAA method.

REFERENCES

1. U.S. Department of Health and Human Services, Agency for Toxic Substances and Disease Registry, Chapman & Hall, New York (2000).
2. G. D. Clayton and F. E. Clayton, *Patty's industrial hygiene and toxicology*, 4th Ed., Wiley-Interscience, New York (1994).
3. R. C. Merritt, *The extractive metallurgy of uranium*, Colorado School of Mines Research Institute, Golden CO (1971).
4. C. K. Gupta and N. Krishnamurthy, *Int. Mater. Rev.*, **5**, 204 (1994).
5. F. Habashi, *Handbook of extractive hydrometallurgy*, Vol. III., Wiley, New York (1997).
6. M. Eskandari Nasab, A. Sam and S. Alamdar Milani, *Hydrometallurgy*, **106**, 141 (2011).
7. M. Eskandari Nasab, A. Sam and S. Alamdar Milani, *J. Radioanal. Nucl. Chem.*, **287**, 239 (2011).
8. K. C. Hughes and R. Singh, *Hydrometallurgy*, **6**, 25 (1980).
9. J. C. B. S. Amaral and C. A. Morais, *Miner. Eng.*, **23**, 498 (2010).
10. T. Sato, *J. Appl. Chem.*, **15**, 489 (1965).
11. J. Marchese and M. Campderrós, *Desalination*, **164**, 141 (2004).
12. R. Klaassen, P. H. M. Feron and A. E. Jansen, *Chem. Eng. Res. Des.*, **83**, 234 (2005).
13. A. Gabelman and S. T. Hwang, *J. Membr. Sci*., **159**, 61 (1999).
14. C. S. Kedari, S. S. Pandit and P. M. Gandhi, *J. Membr. Sci*., **430**, 188 (2013).
15. M. S. Manna, K. K. Bhatluri, P. Saha and A. K. Ghoshal, *J. Membr. Sci*., **447**, 325 (2013).
16. G. Schultz, *Desalination*, **68**, 191 (1988).
17. V. S. Kislik (Ed.), *Liquid membranes: principles & applications in chemical separations & wastewater treatment*, Elsevier, Oxford UK, 401 (2010).
18. W. S. W. Ho and K. K. Sirkar, *Membrane handbook*, Chapman & Hall, New York (1992).
19. N. Leepipatpiboon, U. Pancharoen and P. Ramakul, *Korean J. Chem. Eng.*, **30**, 194 (2013).
20. D. Buachuang, P. Ramakul, N. Leepipatpiboon and U. Pancharoen, *J. Alloys Comp*., **509**, 9549 (2011).
21. P. Ramakul, T. Supajaroon, T. Prapasawat, U. Pancharoen and A. W. Lothongkum, *J. Ind. Eng. Chem.*, **15**, 224 (2009).
22. P. Ramakul, N. Leepipatpiboon, C. Yamoum, U. Thubsuang, S. Bunnak and U. Pancharoen, *Korean J. Chem. Eng.*, **26**, 765 (2009).
23. N. Sunsandee, U. Pancharoen, P. Rashatasakhon, P. Ramakul and N. Leepipatpiboon, *Sep. Sci. Technol.*, **48**, 2363 (2013).
24. N. Sunsandee, N. Leepipatpiboon and P. Ramakul, *Korean J. Chem. Eng.*, **30**, 1312 (2013).
25. G. S. Peace, *Taguchi methods: a hands-on approach*, Addison-Wesley, Reading MA (1993).
26. J. Guervenou, P. Giamarchi, C. Coulouarn, M. Guerda, C. Le Lez and T. Oboyet, *Chemom. Intell. Lab. Syst*., **63**, 81 (2002).
27. J. C. G. E. da Silva, J. R. M. Dias and J. M. C. S. Magalhães, *Anal. Chim. Acta*, **450**, 175 (2001).
28. B. Medjahed, M. A. Didi and D. Villemin, *Desalin. Water Treat*., In Press (2013).
29. D. Kavak, M. Demir, B. Bassayel and A. S. Anagün, *Desalin. Water Treat*., **51**, 1712 (2013).
30. U. Pancharoen, P. Ramakul, W. Patthaveekongka and M. Hronec, *J. Ind. Eng. Chem.*, **12**, 673 (2006).
31. P. N. Pathak, R. Veeraraghavan, D. R. Prabhu, G. R. Mahajan and V. K. Manchanda, *Sep. Sci. Technol.*, **34**, 2601 (1999).
32. J. Stas, A. Dahdouh and H. Shlewit, *Periodica Polytechnica : Chem. Eng*., **49**, 3 (2005).
33. R. B. Bird, W. E. Stewart and E. N. Lightfoot, *Transport phenomena*, 2nd Ed., John Wiley & Sons, New York (2007).
34. D. De Soete, R. Gijbels and J. Hoste, *Neutron activation analysis*, John Wiley & Sons, New York (1972).
35. W. D. Ehmann and D. E. Vance, *Radiochemistry and nuclear methods of analysis*, John Wiley & Sons, New York (1991).
36. Q. Yang and N. M. Kocherginsky, *J. Membr. Sci.*, **297**, 121 (2007).
37. R. A. Robinson and R. H. Stokes, *Electrolyte solutions*, Butterworth, London (1965).
38. E. Mauerhofer, K. Zhernosekov and F. Rösch, *Radiochim. Acta*, **91**, 473 (2003).
39. N. O'Rourke, L. Hatcher and E. J. Stepanksi, *A step-by-step approach to using SAS for univariate & multivariate statistics*, 2nd Ed., SAS Institute, Cary NC (2005).